

● *Original Contribution*

MANIPULATION OF CELLS USING AN ULTRASONIC PRESSURE FIELD

ALBRECHT HAAKE,* ADRIAN NEILD,* DEOK-HO KIM,^{†§} JONG-EUN IHM,[‡] YU SUN,[†]
JÜRIG DUAL,* and BYEONG-KWON JU[§]

*Center of Mechanics and [†]Institute of Robots and Intelligent Systems, Swiss Federal Institute of Technology, Zurich, Switzerland; [‡]Institute for Biological Engineering and Biotechnology, Swiss Federal Institute of Technology, Lausanne, Switzerland; and [§]Microsystem Research Center, Korea Institute of Science and Technology, Seoul, Korea

(Received 2 July 2004, revised 1 March 2005, in final form 8 March 2005)

Abstract—A novel device is described that generates an ultrasonic force field in a fluid layer. The force field arises because of the acoustic radiation force, a second order effect, generated as an ultrasonic wave interacts with a suspended particle. This force field can be used to manipulate objects in the fluid layer trapped between this device and an arbitrary surface, in this case, a flat object slide. The device is shown to be capable of positioning and, in doing so, concentrating human cells to predictable locations. Mesenchymal and HeLa cells were used. Critically, the forces required to do this can be generated by ultrasonic pressure fields that do not affect the viability of the cells. The viability has been assessed using trypan blue dye. The device used consists of a 14 mm square glass plate that is excited by at least one of four piezotransducers attached to the edges. The resulting ultrasonic force field and, importantly, the location of the minima in the force potential at which the cells are collected, has been calculated analytically. (E-mail: adrian.neild@imes.mavt.ethz.ch) © 2005 World Federation for Ultrasound in Medicine & Biology.

Key Words: Standing wave, Manipulation, Positioning, Lamb wave.

INTRODUCTION

A large number of devices using ultrasonic forces have been described in the literature. These forces arise as a second order effect when an ultrasonic wave interacts with a suspended particle. If second order terms are retained, when the pressure is integrated over the surface of the sphere and time-averaged, the result is the acoustic radiation force (King 1934). A substantial portion of these devices are acoustic filters that can partially separate two phases from each other, provided that at least one is liquid or gaseous (Gröschl 1998; Gröschl et al. 1998; Benes et al. 1995). When the particles are located at predetermined positions, the clarified liquid between these positions can be removed separately, leaving the particles in a smaller body of fluid and, so, at a higher concentration. This can be achieved when the direction of the planes where the particles are collected and the direction of the fluid flow of the cleared fluid are oblique (Schram 1990) or parallel (Hawkes and Coakley 1996).

Applications for acoustic filtering often require simple 1-D standing waves. However, to use ultrasonic forces for manipulation or positioning of particles, a more complicated sound field is necessary. It might be spatially 2-D or 3-D or its excitation might be amplitude- or phase-modulated. For example, Bar-matz and Allen (1988) describe an apparatus for levitating an object acoustically. The disadvantage is that the object can only be positioned in this special container. Some applications use a plurality of transducers to form a complex sound field. One possibility is using a line-focused transducer with multiple electrodes. As explained by Kozuka et al. (2000), particles can be transported two-dimensionally. A plurality of ultrasound (US) transducers, functioning independently of each other, was presented by Mitome et al. (2000) and Umemura et al. (2001). The resulting sound field is a superposition of the sound field from each of the transducers. However, for such sound fields, a complex control device is necessary. Each transducer needs its own excitation signal, differing in time, amplitude and waveform. A method to trap a particle with two focused US beams was introduced by Wu

Address correspondence to: Adrian Neild, Institute of Mechanical Systems, CLA H25, ETH Zentrum, Zürich 8092 Switzerland. E-mail: adrian.neild@imes.mavt.ethz.ch

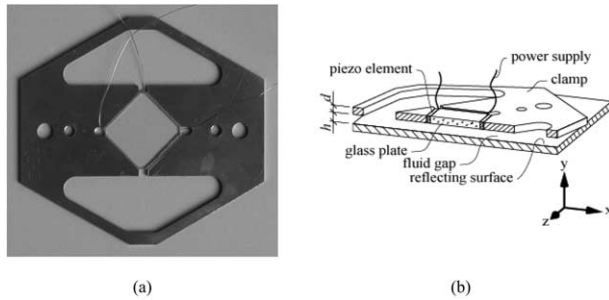


Fig. 1. (a) Photograph of top view and (b) schematic of section view of general setup used for positioning cells. A glass plate is excited by piezoelectric transducers that are glued to each edge. The resulting vibration creates a sound field that applies forces on the particles. Glass-piezo-unit is held by a stainless-steel clamp. Cells suspended in the fluid gap between glass plate and an arbitrary surface can be positioned by the force field.

(1991). The US beams are generated by piezoelectric shells and the particle is trapped in the focal point.

The method described here consists of an active and a passive glass plate, between which a fluid layer is trapped. The active plate is excited by attached piezoelectric elements. This causes the propagation of an asymmetrical plate wave that is reflected at the far end of the glass plate, resulting in a standing wave. The speed of propagation of this plate wave is such that a wave is emitted into the fluid layer; this is reflected by the passive glass plate and the result is a 2-D pressure field and, hence, a 2-D force field in the fluid results. Consequently, cells suspended in this layer are concentrated at specific locations. This novel device is termed a “glass-piezo-unit” and the general setup is shown in Fig. 1. The glass plate measures 14 mm square, with the piezoelements 0.5 mm wide; the thickness of the system, labeled as d in Fig. 1b, is 1 mm. The method described here has the advantage of being simple to operate and requiring just a single drive signal. It requires no special chamber; indeed, it can be located above any surface and so, for example, the passive glass layer (a glass slide in the experiments described here) could be replaced by a silicon wafer. In addition, the force field is established over many wavelengths, allowing parallel handling of cells in multiple lines.

Forces arising from an acoustic field

In this section, only the forces arising from the interaction of the acoustic field with the suspended cells are considered. These can be categorized as three types, primary forces or acoustic radiation force, secondary forces and drag forces because of acoustic streaming. Primary forces arise from the interaction of one object with the surrounding medium, and secondary forces arise between two objects within the medium. In addition,

acoustic streaming is the movement of fluid, usually in rotational patterns, because of the acoustic field; this exerts a force caused by drag (Nyborg 1965). However, experimental work showed that the equilibrium location of the cells can be described without considering streaming and so it is omitted from further discussion.

In the field of suspension separation, such as in acoustic filters, the equations of King (1934) and Yosioka and Kawasima (1955) are frequently used for the calculation of the primary force. It is important to note that, although the forces arise because of second order terms considered at the interface between particle and fluid, the sound field itself can be considered as linear (Yosioka and Kawasima 1955; Gor'kov 1961). However, the equations derived in these two pieces of work apply to a 1-D propagating or standing wave field, which is not the case in the device used here. Consequently, the more general solution for arbitrary acoustic fields developed by Gor'kov (1961) must be used. This states that the time-averaged (indicated throughout by $\langle \rangle$) force is given by:

$$\langle \vec{F} \rangle = -\nabla \langle U \rangle, \quad (1)$$

where $\langle U \rangle$ is the force potential with:

$$\langle U \rangle = 2\pi\rho_f r^3 \left(\frac{1}{3} \frac{\langle p^2 \rangle}{\rho_f^2 c_f^2} f_1 - \frac{1}{2} \langle q^2 \rangle f_2 \right). \quad (2)$$

The terms $\langle p^2 \rangle$ and $\langle q^2 \rangle$ are the mean square fluctuations of the pressure and particle velocity (that is the fluid particles) in the incident wave at the point where the particle is located, $f_1 = 1 - \rho_f c_f^2 / (\rho_s c_s^2)$ and $f_2 = 2(\rho_s - \rho_f) / (2\rho_s + \rho_f)$. The terms ρ_s and ρ_f refer to the density and c_s and c_f to the speed of sound in the objects and fluid, respectively, and r refers to the object radius. For the calculation of $\langle p^2 \rangle$ and $\langle q^2 \rangle$, the linearized equation of the sound field can be used; therefore, $p = \rho_f \partial \phi / \partial t$ and $q^2 = v_x^2 + v_y^2 + v_z^2$, with $v_x = -\partial \phi / \partial x$, etc., ϕ being the velocity potential and, hence, what needs to be found to calculate the force field. The expression given in eqn (2) is valid for compressible spheres in a sound field so that $k_F r \ll 1$, where k_F is the wave number given by dividing the angular frequency, ω , by the speed of sound in the fluid medium.

In addition to the primary force described above, there are various types of secondary forces; these arise from the interaction of two particles within the sound field. The most relevant secondary force, as it applies to compressible particles that would include cells, is the Bjerknes force. For a more complete list, see Gröschl (1998). The Bjerknes force is an attractive force between two particles in a sound field. According to Crum (1970),

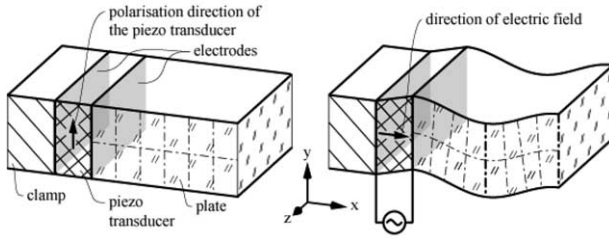


Fig. 2. Arrangement of the piezotransducer and the plate to excite asymmetrical modes. Polarization direction of piezoelectric ceramic is perpendicular to applied electric field, so transducer performs shear deformation.

the time-averaged Bjerknes force acting on one compressible sphere by another can be deduced from:

$$F_{Bj} = -\langle V_s(t) \nabla p(t) \rangle, \quad (3)$$

where V_s is the volume of the particle and p the acoustic pressure. The pressure in the sound field is time-dependent. This causes a change of the volume of the compressible particle. Apfel (1990) gives the Bjerknes force for the case where the wavelength in the fluid is much larger than the particle radius,

$$F_{Bj} = -\frac{2}{9} \pi \frac{\rho_F \omega^2 p^2 r_1^3 r_2^3 (\beta_1 - \beta_F)(\beta_2 - \beta_F)}{d^2}, \quad (4)$$

where ρ_F is the density of the fluid, ω is the angular frequency, r_1 and r_2 are the radii of the two particles, d is their separation distance, β_1 and β_2 are their respective compressibilities and β_F is the compressibility of the fluid. If both particles are made of the same material, then F_{Bj} is always an attractive force and, as such, will aid the gathering of cells at defined locations. Note that eqn (4) does not apply to particles of high gas content and, in that case, the force would not always be attractive.

Theoretical analysis

In Fig. 1, the glass-piezo-unit used to position cells is shown. The key features are the four piezoelements that are attached to the glass plate. When one of these piezoelements is excited by a voltage signal (typically at megahertz frequencies), a shear displacement will occur because of the polarization direction of the elements, as can be seen in Fig. 2. Consequently, the plate will vibrate and a surface vibration propagates along the plate. The nature of this ultrasonic vibration and the relationship between the wavelength and frequency is discussed in detail in Haake and Dual (2004). Here, the resulting force field that occurs in the fluid body trapped between the vibrating plate and the reflecting surface, as shown in Fig. 1, is the focus of consideration. It will be seen that

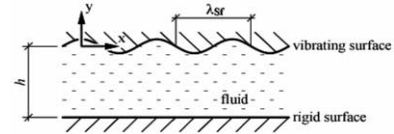


Fig. 3. Arrangement of two surfaces and fluid. Upper surface is drawn performing a 1-D vibration.

this force field is 2-D and so it is only necessary to operate one transducer to position the cells in lines. The motion of the vibrating plate will be treated as a sinusoidal surface displacement of given wavelength λ_{sf} , as shown in Fig. 3 (at 1.2 MHz, this is 2.1 mm).

Initially, the case of a propagating surface wave emitting a sound wave into an adjacent fluid will be considered. The displacement of the surface in the y -direction is given by:

$$u_{sf} = u_{sf0} e^{i(\omega t - k_{sf} x)}, \quad (5)$$

where u_{sf0} is the peak amplitude of the vertical displacement and k_{sf} is the wave number given by $k_{sf} = 2\pi/\lambda_{sf}$. The resultant velocity potential in the fluid, when attenuation is ignored, has the form:

$$\phi = -\Phi e^{i(\omega t - x k_{Fx} + y k_{Fy})}, \quad (6)$$

where the wave numbers k_{Fx} and k_{Fy} , defined, respectively, as the wave number in the x - and y -directions, are related to k_F by $k_F^2 = k_{Fx}^2 + k_{Fy}^2$. The boundary condition is that, at the interface between the plate and fluid ($y = 0$), the velocities in the y -direction of the surface displacement and fluid must be equal, that is,

$$-\frac{\partial \phi}{\partial y} \Big|_{y=0} = \frac{\partial u_{sf}}{\partial t} \Big|_{y=0}. \quad (7)$$

This yields the result that $\Phi = \omega u_{sf0}/k_{Fy}$ and that $k_{Fx} = k_{sf}$, meaning that the fluid wave propagates in the positive x -direction with the same speed as does the surface wave.

For the manipulation of particles, a standing sound field is used because the applied force in an inviscid fluid is orders of magnitude higher than in a propagating wave (King 1934; Yosioka and Kawasima 1955). To achieve this, two modifications to the case of a propagating wave have to be introduced; the surface wave has to be stationary and the fluid wave has to be reflected. The second modification results in the setup shown in Fig. 1, with a reflecting surface at distance h away (also see Fig. 3). The first modification can be achieved by having an additional propagating wave traveling in the opposite direction (*e.g.*, resulting from a reflection). This leads to an additional term in the expression of the surface displacement u_{sf} . The displacement in the y -direction of the

standing surface wave can be written as the sum of the two propagating waves, giving:

$$u_{sf} = \frac{1}{2} u_{sf0} (e^{ik_{sf}x} + e^{-ik_{sf}x}) e^{i\omega t} = u_{sf0} \cos(xk_{sf}) e^{i\omega t}. \quad (8)$$

Because of the reflection of the surface wave and the reflection of the waves propagating in the fluid, the velocity potential in the fluid can be expressed as a sum of four parts:

$$\begin{aligned} \phi = & (\Phi_{+-xy} e^{i(-k_{sf}x + k_{fy}y)} + \Phi_{++xy} e^{i(-k_{sf}x - k_{fy}y)} \\ & + \Phi_{- -xy} e^{i(k_{sf}x + k_{fy}y)} + \Phi_{- +xy} e^{i(k_{sf}x - k_{fy}y)}) e^{i\omega t}. \quad (9) \end{aligned}$$

where the subscripts of the amplitudes Φ refer to the direction of propagation. By consideration of the phase change resulting from the traveling time from the vibrating surface to the reflector and back and using the boundary condition of eqn (7), the velocity potential in the fluid can be found. The result is:

$$\phi = i \frac{\omega u_{sf0} \cos(xk_{fx})}{k_{fy} \sin(hk_{fy})} \cos((h+y)k_{fy}) e^{i\omega t}. \quad (10)$$

To arrive at this analytical result, several simplifications and assumptions have had to be used. First, it is assumed that the coupling of the vibration in the plate with the fluid results in a planar wave propagating at an angle given by $\sin^{-1}(k_{sf}/k_f)$ this is implicit in the relationship of k_{fx} , k_{fy} and k_f , given above. The reflection of the surface wave and the resulting fluid waves are assumed to be ideal. The passive surface is assumed to be rigid. The effect of the finite length of the plate is ignored and the system is considered in two dimensions. In addition, the effect of damping is neglected, although this could be included by the use of complex parameters. Using these simplifications, the location of the nodes of the force field can be calculated using eqn (10).

The velocity potential in the fluid layer can be used to calculate the force potential using $p = \rho_f \partial \phi / \partial t$, $q^2 = v_x^2 + v_y^2 + v_z^2$, where $v_x = -\partial \phi / \partial x$, etc., and eqn (2). This, in turn, can be used to find the forces acting on inhomogeneities within the fluid layer using eqn (1). This calculation has been performed and yields the result:

$$\begin{aligned} \langle F_x \rangle = & U_0 u_{sf0}^2 k_{fx} \sin(2xk_{fx}) \\ & \times \left\{ \begin{aligned} & \frac{f_1}{3} k_f^2 \cos^2((h+y)k_{fy}) \\ & + \frac{f_2}{2} [k_{fx}^2 \cos^2((h+y)k_{fy}) - k_{fy}^2 \sin^2((h+y)k_{fy})] \end{aligned} \right\} \quad (11a) \end{aligned}$$

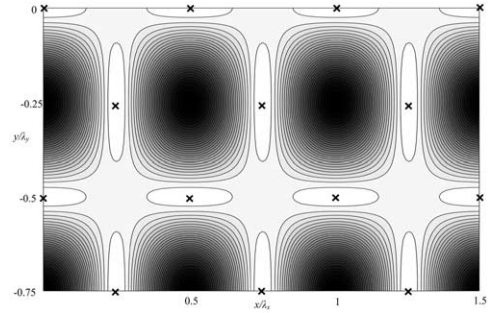


Fig. 4. Force potential in fluid gap for a copolymer sphere in water as a function of spatial variables x and y . Vibrating surface of fluid gap is at $y = 0$ and rigid reflecting surface at $y = -0.75\lambda_{fy}$. Grey scale is used so that black represents maximum force potential. \times = locations of minima of force potential, where particles will settle.

$$\begin{aligned} \langle F_y \rangle = & U_0 u_{sf0}^2 k_{fy} \sin(2(h+y)k_{fy}) \\ & \times \left\{ \begin{aligned} & \frac{f_1}{3} k_f^2 \cos^2(xk_{fx}) \\ & + \frac{f_2}{2} [-k_{fx}^2 \sin^2(xk_{fx}) + k_{fy}^2 \cos^2(xk_{fx})] \end{aligned} \right\} \quad (11b) \end{aligned}$$

where $U_0 = \pi \rho_f \omega^2 r^3 / (k_{fy}^2 \sin^2(hk_{fy}))$ and f_1 and f_2 are as previously given with reference to eqn (2). This result has been used to illustrate the force potential in a fluid layer of thickness $h = 0.75\lambda_{fy}$, as shown in Fig. 4. The figure has contour lines representing equal levels of force potential and is shaded so that maximum force potential is black and minimum is white. The points of minimum force potential are the locations where the particles will collect and are marked with black crosses. It should be noted that the calculation has been performed using values for f_1 and f_2 based on copolymer beads in water. This has been done because the parameters required, the density and speed of sound, are readily available for these materials.

In Fig. 5a, the force potential acting on copolymer beads in water is depicted as calculated, using the model described above when a gap (h) of $200 \mu\text{m}$ is used, as is the case in the experiments described in this work. It can be seen that, when the fluid layer is so thin, the prediction is that the beads will collect at two points per wavelength, again marked by black crosses. This is, however, not supported by experimental work, where a separation equivalent to four points per wavelength is observed, even with such a thin fluid layer. Consequently, an amendment is needed for the model. It has been observed experimentally that the reflector plate moves by a similar amplitude and in both temporal and spatial phases to those of the activated plate. The observation was made by measurement of the outer surface displacements using

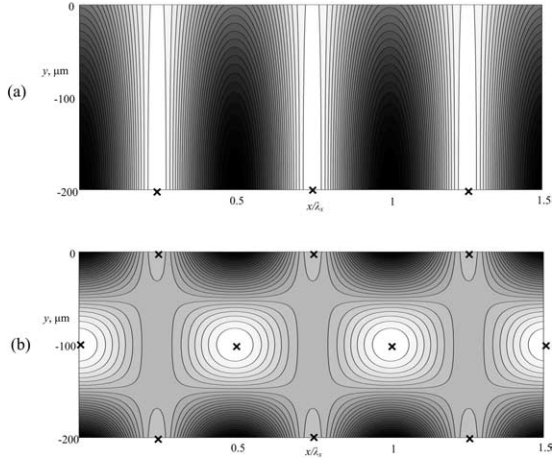


Fig. 5. Force potential in fluid gap for a copolymer sphere in water as a function of spatial variables x and y , when thickness of fluid layer is $200 \mu\text{m}$. Reflecting surface is assumed to be (a) rigid and (b) oscillating. Grey scale is used so that black represents maximum force potential. \times = Locations of minima of the force potential, where particles will settle.

a laser interferometer. The model will now be adapted to account for this. The two plate displacements, that is, for the upper and lower plates, respectively, can be expressed as:

$$u_u = u_{u0} \cos(xk_{Sf})e^{i\omega t}, \quad u_l = u_{l0} \cos(xk_{Sf})e^{i\omega t}, \quad (12)$$

where the terms u_{u0} and u_{l0} refer to the amplitude of the displacement of the upper and lower plates, respectively. The boundary equations for each surface are then:

$$-\frac{\partial \varphi}{\partial y} \Big|_{y=0} = \frac{\partial u_u}{\partial t} \Big|_{y=0} \quad (13a)$$

and

$$-\frac{\partial \varphi}{\partial y} \Big|_{y=-h} = \frac{\partial u_l}{\partial t} \Big|_{y=-h}. \quad (13b)$$

By following the same approach as previously described, the velocity potential is found to be:

$$\varphi = i \frac{\omega \cos(xk_{Fx})}{k_{Fy} \sin(hk_{Fy})} \{u_u \cos((h+y)k_{Fy}) - u_l \cos(yk_{Fy})\} e^{i\omega t}. \quad (14)$$

This results in the forces acting on the inhomogeneities in the fluid being:

$$\langle F_x \rangle = U_0 k_{Fx} \sin(2xk_{Fx}) \times \left\{ \begin{aligned} & \frac{f_1}{3} k_F^2 [u_u \cos((h+y)k_{Fy}) - u_l \cos(yk_{Fy})]^2 \\ & + \frac{f_2}{2} k_{Fx}^2 [u_u \cos((h+y)k_{Fy}) - u_l \cos(yk_{Fy})]^2 \\ & - \frac{f_2}{2} k_{Fy}^2 [u_u \sin((h+y)k_{Fy}) - u_l \sin(yk_{Fy})]^2 \end{aligned} \right\} \quad (15a)$$

$$\langle F_y \rangle = U_0 k_{Fy} [u_u^2 \sin(2(h+y)k_{Fy}) + u_l^2 \sin(2yk_{Fy}) - 2u_u u_l \sin((h+2y)k_{Fy})] \times \left\{ \begin{aligned} & \frac{f_1}{3} k_F^2 \cos^2(xk_{Fx}) \\ & + \frac{f_2}{2} [-k_{Fx}^2 \sin^2(xk_{Fx}) + k_{Fy}^2 \cos^2(xk_{Fx})] \end{aligned} \right\}. \quad (15b)$$

In Fig. 5b, the force potential acting on copolymer beads in water is depicted as calculated using the amended model when a gap (h) of $200 \mu\text{m}$ is used. It can be seen that the resulting force field, using this more realistic assumption about the displacement of the reflecting plate, predicts that there are four points per wavelength, at different heights, again marked with black crosses. Note that, at the positions along $y = 0$ and $y = -h$, the particles experience a force potential gradient that results in a force pushing the particles against the plate so they are at equilibrium.

In Figs. 4 and 5, the lines (extending in the z -direction out of the plane of the diagram) where the inhomogeneities (copolymer particles) collect are shown by black crosses. The location of these minima of the force potential ($\langle U \rangle$) depends on the combination of the material parameters of the fluid and the inhomogeneities. It will be seen later that the cells used and copolymer particles collect in the same location. So, although the amplitude of the forces will differ for the case of cells, the most important result for micromanipulation is that the location will remain the same.

EXPERIMENTAL PROCEDURE AND RESULTS

The drive signal was produced using a signal generator (Krone Hite, KH5920, Avon, MA) connected to the input of a power amplifier (ENI, 2100L, Rochester, NY), the output of which was connected to one of the piezoelements in the device. The movement of the cells in the fluid layer was observed using an inverted microscope (Olympus, IX-81 F-2, Tokyo, Japan), the illumination being from above. The experimental setup is shown in Fig. 6. The fluid layer consisted of a droplet of fluid trapped between the objective slide and glass piezo-unit. The fluid droplet

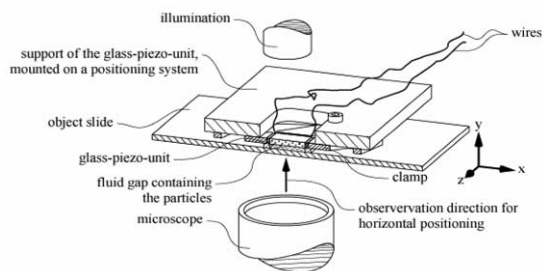


Fig. 6. Detail of experimental setup for cell positioning. Arrangement of glass-piezo-unit and object slide is shown, the cells being located in a fluid layer trapped between the two.

was restricted laterally by glass-walls; the height of these walls defined the fluid layer thickness as $200\ \mu\text{m}$ (parameter h in Fig. 3). Images were taken using a digital camera (Olympus, C5050 Zoom, Tokyo, Japan). The direction of view can be seen to be in the xz plane in Fig. 6. It is important to note that the force field in Fig. 5b is given in the xy plane. The force field is 2-D and is, thus, shown in the two dimensions in which it varies; however, it is not possible to view the system in the same direction. This means that cells are collected at points in the xy plane as predicted in Fig. 5b and so, as will be seen, appear as lines in the xz plane in Figs. 7 to 9.

For the experiments conducted to determine the possibility of positioning cells using the device described above and the viability of the cells, two types of cells were used; these were mesenchymal cells and HeLa cells. The HeLa cell line is a strain that has been continuously cultured since 1951, when the first cells were isolated from a patient suffering from uterine cervical carcinoma. The size of these cancer cells is between $15\ \mu\text{m}$ and $20\ \mu\text{m}$. Mesenchymal stem cells (MSC) are from adult human bone marrow. The bone marrow stroma (connective tissue framework of an organ) consists of a heterogeneous population of cells. Studies have shown that MSC can *inter alia* differentiate into neural cells, skeletal cells and smooth muscle cells. The size of the MSC is between $12\ \mu\text{m}$ and $25\ \mu\text{m}$.

The details of the cell preparation are in Table 1. The mesenchymal cells, the MSC basal medium and the trypsin/EDTA solution used are all products of Cambrex BioScience, Verviers, Belgium. In the experiments, a solution of cells was prepared in a buffer consisting of 25% original medium and 75% deionized water. A $50\ \mu\text{L}$ aliquot of the solution was micropipetted into the millimeter-scale chamber of the ultrasonic device. Deionized water was added to reduce the electrical conductivity because the electrodes of the piezoelements were not insulated. Although this is not ideal for the viability of the cells, what is of interest is the difference

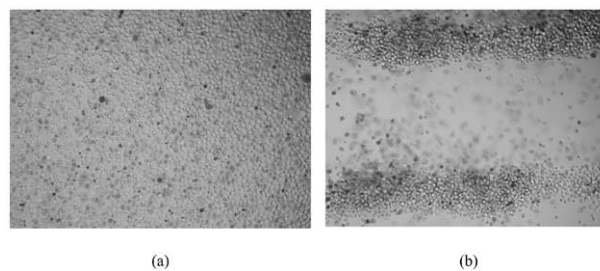


Fig. 7. HeLa cells (a) before and (b) after 160 s of exposure to US field using the same field-of-view.

in the number of live cells caused by the application of the US field. In later stages of device development, the problem of electrode insulation will need to be tackled.

Trypan blue dye was added to the solution containing the cells. This is the most commonly used stain to distinguish between live and dead cells. The nonviable cells appear blue because of absorbing the dye and healthy cells remain unchanged.

Upon application of a sinusoidal voltage of 1.2-MHz frequency and approximately $20\ \text{V}_{\text{r.m.s.}}$ amplitude to a single piezoelement in the device, the cells within the fluid layer formed lines parallel to the activated element. This can be seen in Fig. 7 for the HeLa cells and in Fig. 8 for the mesenchymal cells; the exposure times when the images were made were 160 s and 430 s, respectively. However, it should be noted that clear lines were formed after just 40 s in both cases. The thickness of the lines formed is because of the fairly high concentration of cells within the solution. In Fig. 9, the result from an experiment in which a mixture of mesenchymal cells and $9.6\ \mu\text{m}$ copolymer beads was used can be seen. The beads and cells form lines in the same location, with a higher percentage of the cells being collected than of the beads. In all three cases, the separation has been calculated to be between 0.50 and 0.55 mm.

DISCUSSION

This section will consist of, first, a discussion of the results from the experimental work and what has been

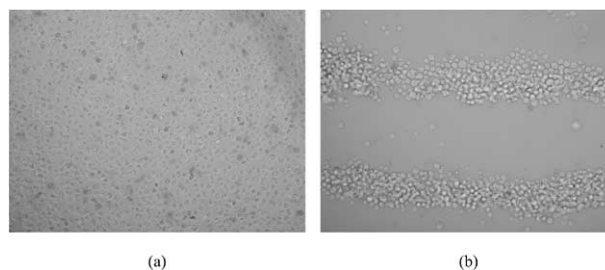


Fig. 8. Mesenchymal cells (a) before and (b) after 430 s of exposure to US field using the same field-of-view.

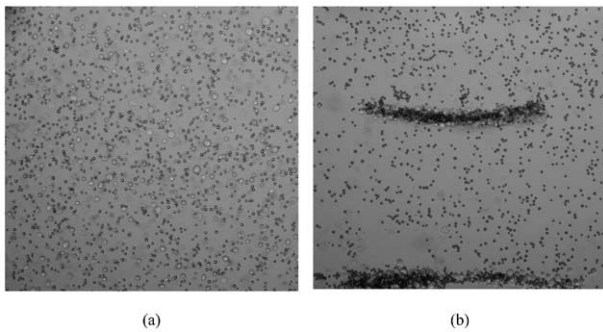


Fig. 9. A mixture of mesenchymal cells and $9.6\ \mu\text{m}$ copolymer beads (a) before and (b) after 180 s of exposure to US using the same field-of-view.

achieved and, then, the advantages of this technique will be considered in comparison with other manipulation techniques.

The aim of this work was to introduce and analytically model a device capable of positioning cells within a 2-D force field so that the cells are moved into lines, without affecting the viability of the cells. The results shown in Figs. 7 and 8 clearly show that the cells can be positioned in lines. To discuss the viability of the cells, a significant parameter, the pressure amplitude in the fluid gap, cannot be given here. It has not been possible to measure the pressure; to calculate it from the known parameters would be highly speculative. Therefore, these experiments cannot give a correlation between the viability and certain measured pressure values or energy densities. However, importantly, the viability can be assessed in relation to a pressure value that is sufficient to displace the particles in the sound field. Other publications dealing with the topic of cell viability had the same problems; for example, they refer to “different power settings, marked 1, 2 and 3” (Sura *et al.* 2001) or to “power delivery settings of approximately 1.5 W or 2.5 W” (Ashokkumar *et al.* 2003).

In all the experiments performed, no significant change in the ratio of the number of alive and dead cells

could be found. Of the two example results shown, this can be most clearly observed in Fig. 8. It can be seen that, before and after application of the ultrasonic field, there are very few dead mesenchymal cells. In addition, it should be noted that the exposure was more than 10 times the length required to position the cells in lines. It can be concluded, from these experiments, that human cells survive the exposure of an US field that is strong enough to position them.

To be able to predict the location of the lines of cells, a further experiment was performed, the result of which is shown in Fig. 9. The locations at which particles are collected are a function of the material parameters of the fluid and particles. The cells and beads are clearly orientated in the same place in the x-direction. This is an important result because it shows that, despite uncertainty about the material properties of the cells used here, the locations at which they are positioned are the same as those for the well-defined copolymer beads and, as such, are predictable. In addition, from this experiment, it can be concluded that the acoustic forces acting on the cells are larger than those acting on the beads; this is because of the difference in radii, which influences the force to the third power.

It has been shown that it is possible to position cells using the device described here. The sound field in the fluid applies forces to the particles and it is possible to position the cells without any contact to solid instruments, bypassing the problem of adhesion and avoiding physical damage. Other methods to manipulate particles or cells include dielectrophoresis, optical tweezers and capillary pipettes.

Dielectrophoresis refers to the force exerted on the induced dipole moment on an uncharged dielectric and/or conductive particle by a nonuniform electric field (Jones 1995), although exposure to electric fields is not always satisfactory.

Ashkin (1970, 1980) indicated that it is possible to accelerate and trap particles by radiation pressure with laser light. By using one laser beam, a particle moves

Table 1. A description of the different steps in the cell preparation

Cell type	Mesenchymal	HeLa
Culture conditions	37°C and 5% CO ₂	37°C and 5% CO ₂
Culture medium	MSCBM containing mesenchymal cell growth supplement, L-glutamine and penicillin/streptomycin	Complete media (MEM- α) containing 10% fetal bovine serum (FBS), L-glutamine and penicillin/streptomycin
Passages	Every 5–6 d, at confluency 80–85%	Every 2–3 d, at confluency 80–85%
Trypsin/EDTA treatment	At passage 4: 10 min, room temperature	At passage 10: 2 min at 37°C and 5% CO ₂
Deactivation of trypsin	Addition of 1 volume of MSCBM	Addition of 10 volume of MEM- α containing 10% FBS
Centrifuge	1200 rpm for 2 min	1200 rpm for 2 min
Resuspension	In MSCBM at final cell number of 2×10^6 cells/mL	In MEM- α containing 10% FBS at a final cell number of 2×10^6 cells/mL

radially to the center of the beam and is accelerated axially in the propagation direction. Thus, a particle can, for example, be pressed against an object slide and then moved on the slide. A particle can also be trapped without contact with another solid in an “optical potential well.” It is created by two coaxial focused laser beams that are positioned in opposite directions with their focal points close to each other. The equilibrium position of a particle lies between the two focal points. Capillary pipettes integrated within microrobotic systems have also been used successfully to manipulate cells (Sun and Nelson 2002).

Although these systems can manipulate single cells sequentially, the method presented here using ultrasonic forces has been shown to be capable of moving numerous cells to many defined locations simultaneously. This advantage arises because the wavelength of US and so the periodicity of the field is much larger than the diameter of the cells used (approximately 2 mm and 20 μm , respectively, in this system) but, for an optical system, the wavelength is in the submicrometer range. In addition, these systems require that the cell is located before manipulation although, in the system presented here, the force field acts over a large volume. This makes this technique suitable for applications where large numbers of cells in undefined locations must be handled, one example being the lining-up of cells in a flow-through device for visual inspection.

CONCLUSIONS

A novel method for manipulating objects within a thin fluid layer has been described and demonstrated by the use of cells. It is clear that this technique can be used to position cells in predictable locations using analytical solutions presented here. The amplitude of the force field is proportional to the cell radius and the frequency, both to the third power, and it is also dependent on the speed of sound and density of both the fluid and the cells suspended within the fluid. In addition, in performing this positioning, no change in the viability of the cells was detected; this was assessed by adding the stain trypan blue to the cell suspension. Because the system has behaved with similar success for cells as has previously been shown for particles, this opens up the possibility of applying other techniques also successfully demonstrated on particles (Haake 2004), such as 3-D positioning and defined micrometer-scale displacement, using the same device as described here to the manipulation of biologic material.

Acknowledgements—This work was supported by KTI/CTI, Switzerland, under a Top Nano 21 grant (project numbers 6643.1 and 6989.1). In addition, Deok-Ho Kim was supported by the International Research Internship Program of the Korea Science and Engineering Foundation (KOSEF) (contract number M07-2003-000-10015-0) and by the 21st Century’s Frontier R&D Projects, sponsored by the Ministry of Science and Technology, Korea. The authors thank Jeffrey A. Hubbell, Institute for Biologic Engineering and Biotechnology, Swiss Federal Institute of Technology, Lausanne, Switzerland, and Brad Nelson, Institute of Robots and Intelligent Systems, Swiss Federal Institute of Technology, Zurich, Switzerland, for their encouragement and comments regarding this work.

REFERENCES

- Apfel RE. Acoustic radiation pressure—Principles and application to separation science. Proceedings of the Fortschritte der Akustik-DAGA’90 Conference, Bad Honnef, Germany: DPG-GmbH, 1990; 19–36.
- Ashkin A. Acceleration and trapping of particles by radiation pressure. *Phys Rev Lett* 1970;24:156–159.
- Ashkin A. Applications of laser radiation pressure. *Science* 1980;210:1081–1088.
- Ashokkumar M, Vu T, Grieser F, et al. Ultrasonic treatment of *Cryptosporidium* oocysts. *Water Sci Technol* 2003;47:173–177.
- Barmatz MB, Allen JL. Single mode levitation and translation. US Patent 4,736,815. April 12, 1988.
- Benes E, Burger W, Groeschl M, Trampler F. Method for treating a liquid. EP Patent 0 633 049 A1. January 11, 1995.
- Crum LA. Acoustic force on a liquid droplet in a stationary sound field. *J Acoust Soc Am* 1970;47:82.
- Gor’kov LP. Forces acting on a small particle in an acoustic field within an ideal fluid. *Doklady Akad Nauk Sssr* 1961;140:88–92.
- Gröschl M. Ultrasonic separation of suspended particles—Part I: Fundamentals. *Acustica* 1998;84:432–447.
- Gröschl M, Burger W, Handl B. Ultrasonic separation of suspended particles—Part III: Application in biotechnology. *Acustica* 1998; 84:815–822.
- Haake A. Micromanipulation of small particles with ultrasound. Ph.D. Thesis. ETH Zürich, 2004.
- Haake A, Dual J. Positioning of small particles by an ultrasound field excited by surface waves. *Ultrasonics* 2004;42:75–80.
- Hawkes JJ, Coakley WT. A continuous flow ultrasonic cell-filtration method. *Enzyme Microb Technol* 1996;19:57–62.
- Jones TB. *Electromechanics of particles*. Cambridge: Cambridge University Press, 1995.
- King LV. On the acoustic radiation pressure on spheres. *Proc Roy Soc London (Ser A)* 1934;147:212–240.
- Kozuka T, Tuziuti T, Mitome H, Fukuda T. Micromanipulation using a focused ultrasonic standing wave field. *Electron Commun Jpn (Part Iii)* 2000;83:53–60.
- Mitome H, Kozuka T, Tuziuti T. Non-contact micromanipulation method and apparatus. US Patent 6,055,859. May 2, 2000.
- Nyborg WL. Acoustic streaming. In: Mason WP, ed. *Physical acoustics*. Vol. 2. Part B. New York: Academic Press, 1965:265–331.
- Schram CJ. Controlling particulate material. EP Patent 0 380 194 A1. August 2, 1990.
- Sun Y, Nelson BJ. Biological cell injection using an autonomous microrobotic system. *Int J Robotics Res* 2002;21:861–868.
- Sura H, Shelton RM, Walmsley AD. Osteoblast viability and detachment following exposure to ultrasound in vitro. *J Materials Sci Materials Med* 2001;12:997–1000.
- Umamura SI, Kamahori M, Sasaki K, et al. Particle handling apparatus for handling particles in fluid by acoustic radiation pressure. US Patent 6,216,538. April 17, 2001.
- Wu JR. Acoustical tweezers. *J Acoust Soc Am* 1991;89:2140–2143.
- Yosioka K, Kawasima Y. Acoustic radiation pressure on a compressible sphere. *Acustica* 1955;5:167–173.